

Structure, Expression and Chromosome Mapping of *MLZE*, a Novel Gene Which Is Preferentially Expressed in Metastatic Melanoma Cells

Kenji Watabe,¹ Akihiko Ito,² Hideo Asada,³ Yuichi Endo,⁵ Toshiko Kobayashi,⁶ Ken'i Nakamoto,¹ Satoshi Itami,³ Sonshin Takao,⁷ Yasuhisa Shinomura,⁴ Takashi Aikou,⁷ Kunihiko Yoshikawa,³ Yuji Matsuzawa,⁴ Yukihiko Kitamura² and Hiroshi Nojima^{1,8}

¹Department of Molecular Genetics, Research Institute for Microbial Diseases, Osaka University, 3-1 Yamada-oka, Suita, Osaka 565-0871, Departments of ²Pathology, ³Dermatology, ⁴Internal Medicine and Molecular Science, Osaka University Medical School, 2-2 Yamada-oka, Suita, Osaka 565-0871, ⁵Department of Biochemistry, Fukushima Medical College, 1 Hikarigaoka, Fukushima, Fukushima 960-1247, ⁶Ina Laboratories, MBL Co., Ltd., 1063-103 Ohara, Terasawaoka, Ina, Nagano 396-0002 and ⁷First Department of Surgery, Kagoshima University School of Medicine, 8-35-1 Sakuragaoka, Kagoshima 890-8520

We isolated a novel gene, termed *MLZE*, from a B16-BL6 cDNA library after subtraction of B16-F10 mRNA. Expression levels of mouse *MLZE* (*mMLZE*) increased in accordance with metastatic ability of B16 melanoma sublines. Human homolog of *mMLZE* (*hMLZE*) contained one leucine zipper structure and two potential nuclear localizing signals. Northern blot analysis of multiple human tissues showed that *hMLZE* was expressed primarily in trachea and spleen. We mapped the *hMLZE* gene (by fluorescence *in situ* hybridization) to 8q24.1–2, which contains the *c-myc* gene and is often amplified in malignant melanoma. Immunohistochemistry revealed that the number of *hMLZE*-positive cases was significantly larger in Clark levels III, IV and V melanomas (6/11=55%) than in Clark levels I and II melanomas (2/15=13%). In two cases of *hMLZE*-positive melanomas, the strength of *hMLZE* staining increased substantially in the deep component of the tumor. Considering that melanomas above Clark level II are more metastatic than those below Clark level III, these findings suggested that *MLZE* is one of the genes whose expression is upregulated during the course of acquisition of metastatic potential in melanoma cells.

Key words: B16 melanoma — *c-myc* — Metastasis — Tumor progression — Subtraction

The incidence of cutaneous melanoma has increased at an alarming rate throughout the world.¹⁾ Most thin melanomas can be cured by surgical excision. However, once metastases are formed, the disease is rarely curable and median survival time is approximately 6 months.²⁾ There seems to be a difference between thin and more advanced melanoma with respect to their clinical behaviors. Based on the observation of melanoma spread into the dermis, two phases of melanoma development have been described.³⁾ In the first phase, melanoma cells show intraepidermal proliferation and invasion of the papillary dermis by small nests. This phase is defined as the radial growth phase (RGP). In the second phase, melanoma cells gain the capacity to form an expansile nodule in the papillary dermis and infiltrate the reticular dermis and subcutaneous fat. This phase is defined as the vertical growth phase (VGP). By using a mouse model, VGP melanoma cells were shown to possess larger capability of metastasis

than RGP melanoma cells.⁴⁾ In the course of tumor progression from RGP to VGP melanoma, genetic changes may occur that render melanoma cells metastatic. However, few such genetic changes have been identified yet.^{5,6)}

Among the commonly used parameters for the depth of tumor are Breslow thickness⁷⁾ and Clark invasion level.³⁾ Breslow thickness measures the linear depth of tumor in millimeters. It disregards the histological architecture in and around the tumor. In contrast, Clark invasion level describes five invasion levels based on the histologic depth of tumor invasion. Melanomas of level I proliferate within the dermis. Level II melanomas infiltrate the papillary dermis as small nests. Level III melanomas form an expansile nodule that compresses the reticular dermis. Level IV and V melanomas infiltrate into the reticular dermis and subcutaneous fat, respectively. In clinical cases, melanoma cells of level III have been reported to behave in a more malignant manner than melanoma cells of level II.⁸⁾ Clark level II melanomas that carry no systemic metastasis at diagnosis yield a good survival of 96% after 8 years. In contrast, 8-year survival drops markedly to 76% when melanoma cells have already invaded to the depth of level III at diagnosis. Although Clark invasion level is a histologic classification, it is reasonable to con-

⁸To whom all correspondence should be addressed.

E-mail: hnojima@biken.osaka-u.ac.jp

Sequences reported herein have been submitted to the DDBJ/GenBank/EMBL database under the accession numbers AB042405 (*hMLZE* cDNA) and AB042406 (*mMLZE* cDNA).

sider that Clark level I and II melanomas correspond to RGP, and melanomas above Clark level II correspond to VGP.

In the present study, we attempted to characterize a novel gene, termed *MLZE* (Melanoma-derived Leucine Zipper, Extra-nuclear factor), as a marker for melanoma progression from RGP to VGP. To isolate *MLZE*, we examined a pair of B16 mouse melanoma cells, B16-F10 cells⁹⁾ and B16-BL6 cells.¹⁰⁾ B16-BL6 cells were obtained through six rounds of *in vitro* selection of B16-F10 cells. When injected into footpad, B16-BL6 cells metastasize to the lung at high frequency, whereas B16-F10 cells do not. With an improved method for constructing a subtracted cDNA library,¹¹⁾ we have isolated a series of genes that were transcriptionally upregulated in B16-BL6 cells as compared with B16-F10 cells.^{12–15)} *MLZE* was one such gene. Expression levels of *mMLZE* increased as B16 melanoma cells become more metastatic. Human homolog of *mMLZE* (*hMLZE*) contained one leucine zipper structure and two potential nuclear localizing signals (NLS). Immunohistochemistry revealed that the number of *hMLZE*-positive cases were larger in Clark levels III, IV and V melanomas than in Clark levels I and II melanomas. In some cases, the strength of *hMLZE* immunostaining increased substantially at the deep component of the tumor. *hMLZE* may be one of the genes whose expression is upregulated as malignant melanoma progresses from RGP to VGP.

MATERIALS AND METHODS

Cell lines F1, F10, and BL6 mouse melanoma cells were kindly provided by I. J. Fidler (The University of Texas, Houston, TX). Melan-a mouse melanocyte cells were kindly provided by D. C. Bennett (St. Georges Hospital Medical School, Cranmer Terrace, London, UK).¹⁶⁾ 293T human embryonic kidney cells and COS-7 monkey embryonic kidney cells were purchased from American Type Culture Collection (Manassas, VA). Melan-a cells were maintained in Dulbecco's modified Eagle's medium (DMEM) supplemented with 10% fetal calf serum and 200 nM 12-*O*-tetradecanoylphorbol-13-acetate (TPA). The remainder were maintained in DMEM supplemented with 10% fetal calf serum.

Screening of cDNA and genomic DNA libraries Preparation of subtracted cDNA library was performed as described previously.¹¹⁾ To obtain *hMLZE*, a human cDNA library was prepared from HeLa cells using the λ ZAP-cDNA synthesis kit (Stratagene, La Jolla, CA). A total of 1×10^6 clones were screened with a radiolabeled EST clone AW276035 which was obtained by polymerase chain reaction (PCR), and the insert cDNAs were excised from positive clones *in vivo* into pBluescript SK(-) vector. A human placental genomic DNA library was purchased from TaKaRa (Ohtsu) and a total of 1×10^6 clones

were screened with the radiolabeled *hMLZE* coding region.

***In vitro* transcription/translation** The TNT T7 quick coupled transcription-translation system (Promega, Madison, WI) was used according to the manufacturer's instructions.

Northern blot analysis Total RNA was prepared using a guanidine thiocyanate/CsTFA method. For northern blot analysis, 20–30 μ g of total RNA was separated by denaturing gel electrophoresis and transferred to Biodyne A (Pall, Port Washington, NY). Human multiple tissue northern blots were purchased from Clontech, Palo Alto, CA. The *hMLZE* coding region, amplified by PCR with the primer set F-*hMLZE* (5'-ATGCCCTCCATGTTGGAACG-3') and R-*hMLZE* (5'-TTAGGCCTCAGCCAGCTGCT-3'), was radiolabeled with [α -³²P]dCTP using a Random Primer DNA Labeling Kit (TaKaRa).

Fluorescence *in situ* hybridization (FISH) The partial genomic DNA of *hMLZE* was obtained by screening a human placental genomic DNA library with the radiolabeled *hMLZE* coding region as a probe. Positive clones were digested with *EcoRI* and a 7-kb fragment was obtained. We confirmed that the fragment contained the sequence of nucleotides 1613–1735 of *hMLZE* cDNA by PCR with the primer set F-G (5'-AGTACGAAATTC-CGAAATGGTAGG-3') and R-G (5'-CTGGTTTAACTTCATATCATTGGA-3'). FISH analysis of R-banded human chromosomes was performed as described previously.¹⁷⁾ Briefly, 150 ng of biotin-labeled genomic DNA probe was hybridized to metaphase chromosome spreads. For fluorochrome detection, the slides were incubated with fluorescein isothiocyanate (FITC)-conjugated avidin (Vector Laboratories, Burlingame, CA) and then washed. The FITC signals were amplified by incubation with biotin-conjugated goat anti-avidin antibody (Vector Laboratories) followed by incubation with FITC-conjugated avidin. Preparations were counterstained with propidium iodide and observed under a laser scanning microscope (Zeiss LSM410).

Generation of anti-*hTib23* antibody A modified pET28a vector (Novagen, Madison, WI) was constructed by replacing the multiple cloning sites of pET28a with that of pET32a (Novagen) at the *BamHI*-*TthIII* sites. This modification allowed the insertion of cDNA by way of the *BamHI*-*NotI* sites. Using the pBluescript SK(-) vector containing the full-length *hMLZE*, PCR was performed with the following set of primers: F-*Bam*-*hMLZE*, 5'-GGA-TCCATGCCCTCCATGTTGGAACG-3'; R-*Not*-*hMLZE*, 5'-GCGGCCGCTTAGGCCTCAGCCAGCTGCT-3'. The PCR-amplified cDNA fragment was subcloned into the pT7 Blue vector (Novagen). The amplified cDNA fragment was excised and ligated into the modified pET28a vector by way of the *BamHI*-*NotI* sites. The plasmid was transformed to BL21-CodonPlus (Stratagene) and expres-

sion of the 6 His-tagged hMLze was induced with 0.2 mM isopropylthiogalactoside. The bacteria were lysed by sonication and hMLze tagged with 6 His was extracted from the insoluble pellet with 8 M urea, 0.5 M NaCl, 5 mM imidazole and 20 mM Tris-HCl (pH 8.0). Extracted protein was applied to Talon resin and eluted with excess imidazole. White rabbits were immunized with the purified protein to produce polyclonal antibody.

Western blot analysis Whole cell lysates were prepared by adding 10 times the volume of lysis buffer (50 mM Tris-HCl [pH 8.0], 250 mM NaCl, 0.1% NP-40, 1 mM phenylmethylsulfonyl fluoride (PMSF)) to a pellet of 1×10^6 cells. The lysate (50 μ g of protein) was boiled for 5 min, separated on 10% SDS-polyacrylamide gel electrophoresis (PAGE) gel and transferred onto Immobilon membrane (Millipore, Eschborn, Germany). The membrane was incubated with rabbit anti-hMLze polyclonal antibody at 1:200 dilution or rabbit anti-GFP polyclonal antibody (MBL, Nagoya) at 1:1000 dilution for 1 h, then incubated with horseradish peroxidase-conjugated anti-rabbit IgG antibody at 1:1000 dilution (MBL). For detection of the immunocomplex, Renaissance chemiluminescence reagent (Dupont/NEN, Boston, MA) was used.

Immunohistochemistry Formalin-fixed and paraffin-embedded specimens were deparaffinized and hydrated in a graded series of alcohols. Endogenous peroxidase was quenched in phosphate-buffered saline containing 0.3% peroxide. The samples were incubated with anti-hMLze polyclonal antibody at 1:200 dilution or anti-c-Myc monoclonal antibody (Ab-1, Oncogene Science, Cambridge, MA) at 1:100 dilution for 2 h at room temperature, followed by incubation with horseradish peroxidase-conjugated anti-rabbit IgG antibody or anti-mouse IgG₁ antibody (MBL) for 1 h at room temperature. Thereafter, the final products were visualized using diaminobenzidine (DAB) or aminoethylcarbazole (AEC) as a substrate for peroxidase. Negative controls were run with using non-immunized rabbit IgG instead of the primary antibody. The slides were counterstained with Mayer's hematoxylin.

Immunocytochemistry Cells were plated on chamber culture slides (Becton Dickinson, Franklin Lakes, NJ). Cells were fixed with 4% paraformaldehyde in phosphate-buffered saline (PBS), permeabilized with 0.1% Triton X-100 in PBS, blocked with 2% bovine serum albumin (BSA) in PBS, incubated with anti-hTib23 antibody at 1:200 dilution at room temperature for 2 h, and stained with FITC-labeled anti-rabbit IgG. Cells were visualized with using a confocal laser scanning microscope (Zeiss LSM410).

In vivo analysis of GFP fusion proteins We previously reported a modified pEGFP-C1 vector (Novagen), termed pEGFP3B.¹⁸⁾ This vector allowed the cDNA insert to be fused to the 3' end of EGFP by way of *AscI*-*NotI* sites. We also reported a modified pEGFP3B vector, termed pEGFP3 vector. This vector was constructed by insertion

of an in-frame stop codon between EGFP and the *AscI* site so that it produced EGFP protein and could serve as a control vector for pEGFP3B vector. Using the pBluescript SK(-) vector containing the full-length cDNA for hMLZE as a template, PCR was performed with the following sets of primers: F-*AscI*-hMLZE (5'-GGCGCGCCGATGCCCTCCATGTTGGAACG-3') and R-*NotI*-hMLZE (5'-GCGGC-CGCTTAGGCCTCAGCCAGCTGCT-3') for pEGFP3B-hMLZE; F-*AscI*-NLS2 (5'-GGCGCGCCGAGAGTCTCAGAGTGAAGAA-3') and R-*NotI*-TAA-NLS2 (5'-GCGGCCGCTTAAATGGCTTTCTCCTTGATAACCA-3') for pEGFP3B-hMLZE-NLS2; F-*AscI*-hMLZE and R-*NotI*-TAA- Δ N (5'-GCGGCCGCTTATTCGAAATTTCTGACTCAT-3') for pEGFP3B-hMLZE- Δ N; F-*AscI*- Δ C (5'-GGCGCGC-CGATGGTAGGCTACTGTGCTGC-3') and R-*NotI*-hMLZE for pEGFP3B-hMLZE- Δ C. PCR-amplified DNA fragments were subcloned into the pT7 Blue vector. After amplification, cDNA fragments were excised and ligated into the pEGFP3B vector in-frame by way of the *AscI*-*NotI* sites. The following are the amino acid (a.a.) residues of hMLze protein in each vector intended to be fused to EGFP protein: a.a. residues 1-508, pEGFP3B-hMLZE; a.a. residues 196-227, pEGFP3B-hMLZE-NLS2; a.a. residues 1-246, pEGFP3B- Δ N; a.a. residues 247-508, pEGFP3B- Δ C.

293T cells and COS-7 cells were transiently transfected using Lipofectamine transfection reagent (Gibco-BRL, Gaithersburg, MD). The cells were cultured in 35 mm glass-bottomed culture dishes for 24 h after transfection and then observed *in vivo* through an inverted laser scanning microscope (Zeiss LSM410).

Human malignant melanoma and nevus samples

Twenty-six patients with malignant melanoma and five patients with nevus underwent surgical excision in the Osaka University Hospital. Surgical samples were fixed in formalin and embedded in paraffin.

RESULTS

Isolation of mouse and human MLZE cDNAs Among the cDNA clone pool obtained after subtraction of the B16-BL6 cDNA library with B16-F10 mRNA,¹²⁾ we isolated a mouse novel gene that we termed mouse *MLZE* (*mMLZE*). Expression of *mMLZE* mRNA was detected easily in both B16-F10 and B16-BL6 cells, but it was three-fold stronger in B16-BL6 cells. In contrast, the expression of *mMLZE* was below the limit of detection in melan-a and B16-F1 cells (Fig. 1). Since melan-a cells are non-tumorigenic, and since B16 sublines, F1, F10 and BL6 cells acquire larger potentials for metastasis in this order, expression levels of *mMLZE* correlated well with metastatic potentials of melanoma cells. By screening a B16-BL6 cDNA library, we isolated a 2191-bp-long clone. This clone appeared to carry an almost full-length cDNA

for *mMLZE*, because the *mMLZE* transcript was detectable as a single band of about 2.4 kb in B16-BL6 cells (Fig. 1). *mMLZE* contained an open reading frame of 1570 nucleotides (DDBJ/GenBank/EMBL database accession number AB042406) and was supposed to encode a protein of 468 amino acid residues.

Homology searching at the National Center for Biotechnology Information (NCBI) (<http://www.ncbi.nlm.nih.gov/BLAST/>) revealed that the coding region of *mMLZE* was 79.2% and 81.2% homologous to human EST clones AW276035 and AI05243, respectively. We speculated that these EST clones might constitute a part of the human homolog (*hMLZE*) of *mMLZE*. A HeLa cDNA library was screened for cloning of a full-length *hMLZE* by using AW27635.1 DNA fragment as a probe. Of the positive clones obtained, the longest was 2761-bp long (DDBJ/GenBank/EMBL database accession number AB042405). We estimated it to be nearly full-length, since northern blot analysis showed that the transcript size of *hMLZE* is about 2.8 kb in HeLa cells (data not shown).

The clone contained a 1527 bp open reading frame which encoded a putative protein of 508 amino acid residues with a calculated molecular mass of 57 kDa (Fig. 2). The sequence surrounding the proposed starting codon partially matched the consensus for a eukaryotic translation initiation site.¹⁹⁾ A protein of approximately 60 kDa was generated when the longest clone was subjected to *in vitro* transcription-translation analysis (data not shown), indicating that the predicted start codon was functional *in vitro*. The predicted protein showed no obvious homology to previously identified proteins. However, particular

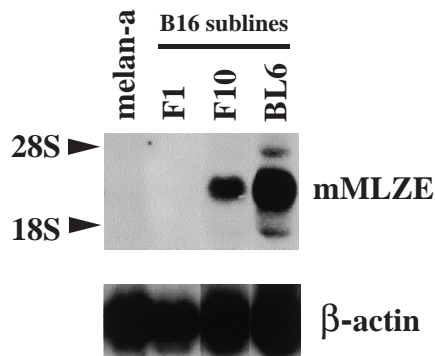


Fig. 1. Northern blot analysis of mouse *MLZE* in melanocyte lineage cells. Northern blot containing 20 μ g of total RNA derived from melan-a cells and B16-F1 cells, B16-F10 cells and B16-BL6 cells was hybridized with ³²P-labeled *mMLZE* cDNA (upper panel). Blots were reprobbed with a mouse β -actin probe, which served as a loading control (lower panel). A transcript of about 2.4 kb was detected abundantly in B16-BL6 cells and moderately in B16-F10 cells, whereas no transcript was detected in melan-a cells and B16-F1 cells.

structural features were identified in the deduced amino acid sequence of *hMLZE*. The N-terminal region was rich in basic amino acids. In particular, amino acid residues 133–151 (KRKLLDPEPSFLKECR) and 201–218 (KKALTLQKGMVMAYKRK) matched the bipartite nuclear localizing signal (NLS) motif.²⁰⁾ The C-terminal region contains a region rich in leucine, including a leucine zipper structure at amino acid residues 392–413.

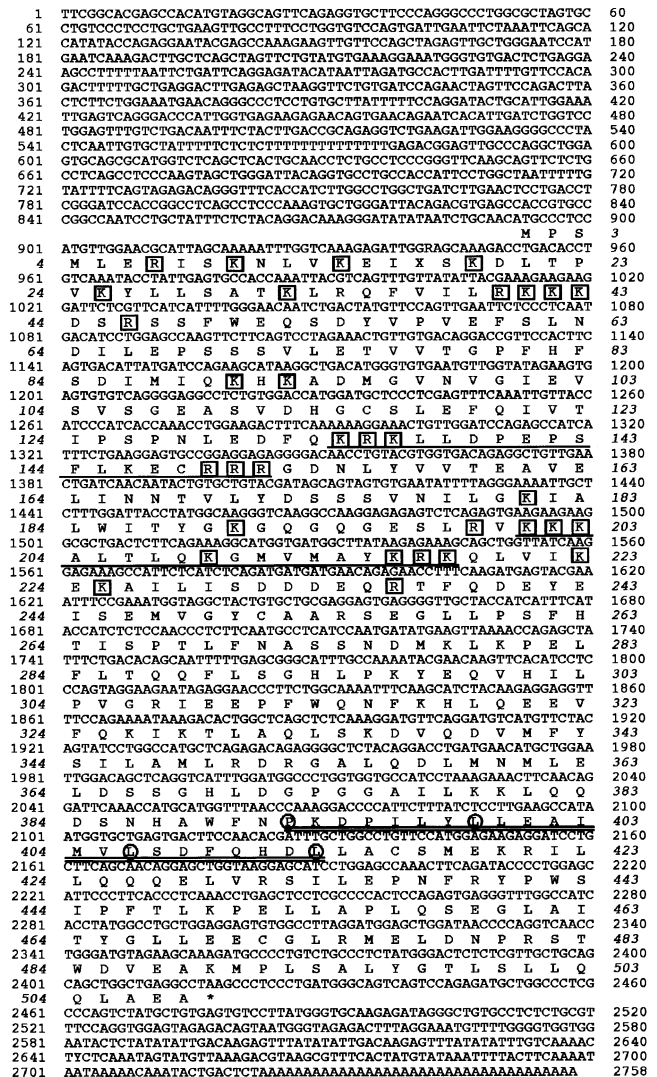


Fig. 2. Identification of human *MLZE*. Nucleotide sequence of the human homolog of mouse *MLZE* (*hMLZE*) and the putative amino acid sequence of the *hMLZE* protein. Structural and sequence elements are indicated as follows: boxes, basic amino acids residues; underlines, bipartite nuclear localizing signals; double underline, a leucine zipper structure; circles, four hydrophobic amino acid residues that constitute a leucine zipper motif; asterisk, a stop codon.

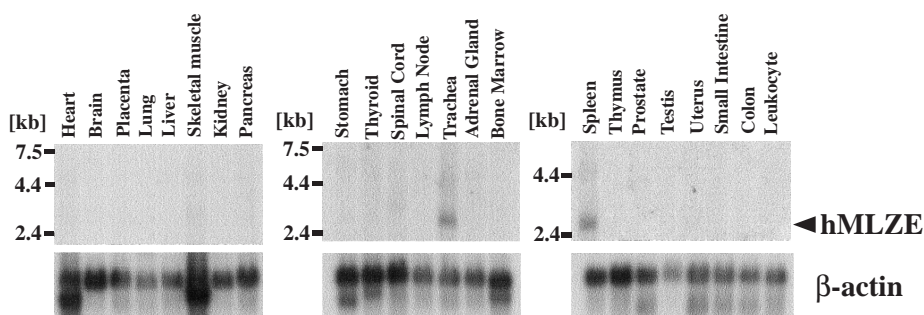


Fig. 3. Northern blot analysis of *hMLZE* in human normal tissue. Human multiple tissue northern blot panel containing around 2 μ g of poly(A)⁺ RNA per lane was hybridized to ³²P-labeled *hMLZE* (upper panel). A transcript of about 2.8 kb was detected weakly in trachea and spleen. The amount of RNA loaded in each lane was normalized using a human β -actin probe (lower panel).

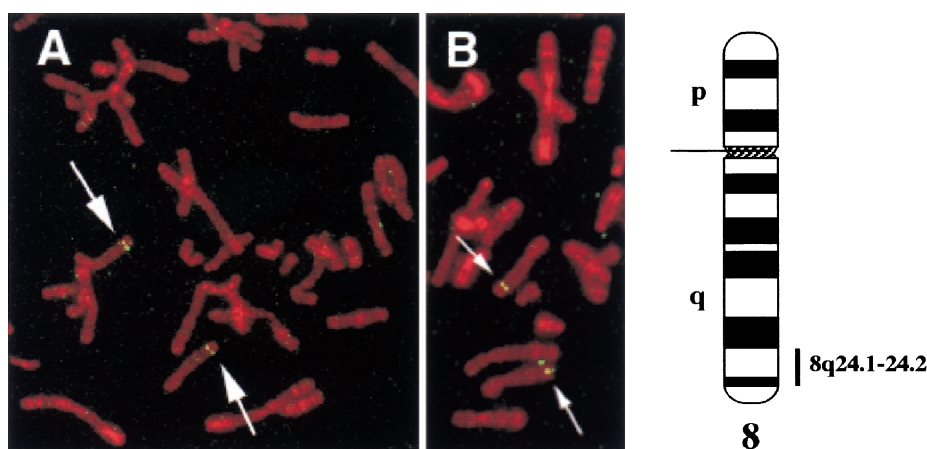


Fig. 4. Chromosomal localization of *hMLZE* gene as detected by FISH. FISH analysis of R-banded chromosomes was performed using a biotinylated *hMLZE* genomic fragment as a probe. Photographs of the entire metaphases (A) and partial metaphases (B) are shown. Separate images of FITC hybridization signals and propidium iodide-stained chromosomes were merged using image analysis software. Arrows indicate specific FITC signals on the long arm of chromosome 8. A schematic representation of human chromosome 8 and the localization of the *hMLZE* gene are shown on the right.

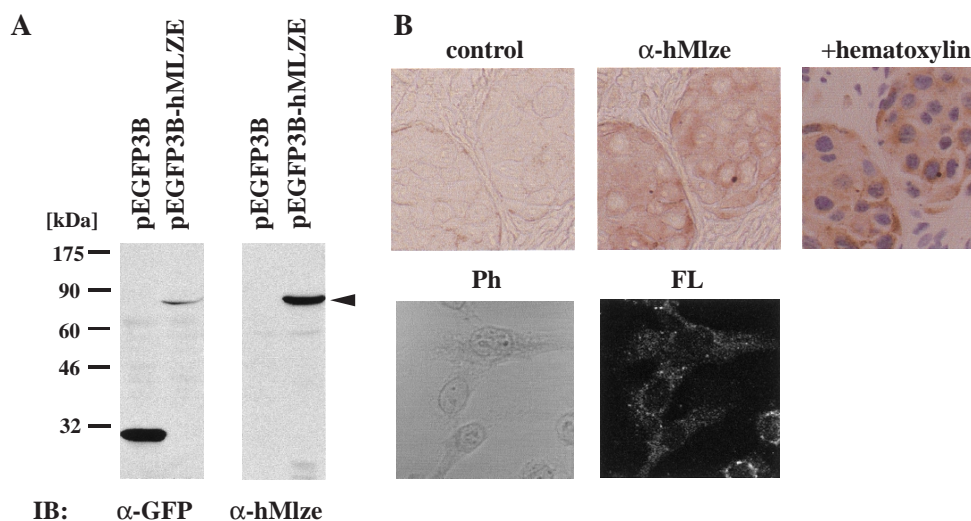


Fig. 5. Immunostaining of B16-BL6 cells using anti-hMLZE antibody. A, evaluation of anti-hMLZE antibody. 293T cells were transiently transfected with pEGFP3B empty or pEGFP3B-hMLZE vector and subjected to immunoblotting. Anti-hMLZE antibody (α -hMLZE) recognized the GFP (27 kDa)-fused hMLZE (57 kDa) protein (arrow). B, immunostaining of hMLZE using anti-hMLZE antibody. A B16-BL6-metastasizing colony was stained with anti-hMLZE antibody (upper panel, middle). The control was run using non-immunized IgG (upper panel, left). Immunostained samples were counterstained with hematoxylin (upper panel, right). Cultured B16-BL6 cells were also immunoreacted with anti-hMLZE antibody and stained with FITC (lower panel). The fluorescence image is shown on the right (FL) and a phase contrast image for the same sample is shown on the left (Ph).

Tissue distribution and chromosomal localization of hMLZE The tissue distribution of hMLZE mRNA was determined by northern blot analysis of a multiple human tissue blot. A transcript of approximately 2.8 kb was detected predominantly in trachea and spleen (Fig. 3).

The chromosomal location of hMLZE gene was determined by FISH analysis. As shown in Fig. 4, specific FISH signals generated from a biotinylated hMLZE genomic DNA fragment were observed at the telomeric region of the long arm of human chromosome 8. No other reproducible signal was observed on metaphase chromosomes. Thus, we concluded that hMLZE gene maps to the 8q24.1–2 region.

Cytoplasmic localization of hMlze By using the anti-

sera against recombinant hMlze, western blot analysis was performed on extracts of 293T cells which had been transiently transfected with pEGFP3 empty vector or pEGFP3B-hMLZE vector. Expression of GFP alone and GFP-tagged hMlze in 293T cells was confirmed with anti-GFP antibody (Fig. 5A). After stripping, the blot was reacted with the anti-hMlze antisera. GFP-tagged hMlze alone was recognized with the antisera. This recognized band disappeared when the reaction was subject to competition with an excess amount of the antigenic recombinant protein (data not shown). Thus, we judged that the antisera could be used as a specific antibody for hMlze.

When the B16-BL6-metastasizing colony was stained with anti-hMlze antibody, cytoplasmic staining was

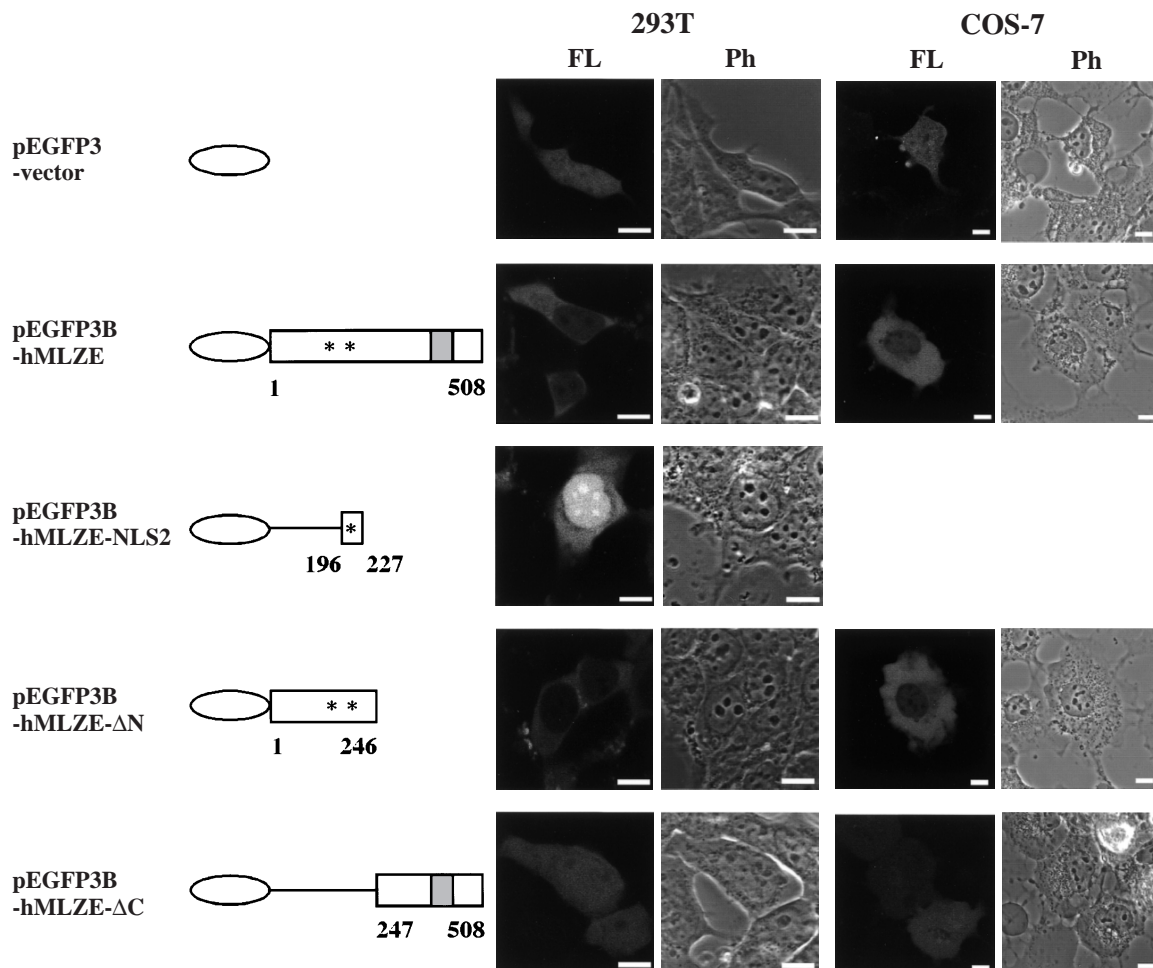


Fig. 6. Subcellular localization study of hMlze using GFP constructs. The left-most illustrations show schematic representations of the GFP fusion proteins used for the expression in 293T and COS-7 cells. The numbers below the boxes indicate the amino acid residues in the hMlze protein. Oval, GFP protein. Asterisk, potential nuclear localizing signal. Grey box, leucine zipper structure. 293T and COS-7 cells were transiently transfected with each fusion construct and observed *in vivo* by fluorescence microscopy after 24 h. The columns shown by FL and Ph represent fluorescence and phase-contrast images, respectively. Scale bar, 10 μ m.

observed in B16-BL6 cells (Fig. 5B). Cultured B16-BL6 cells also showed a cytoplasmic staining (Fig. 5B). The staining in BL6 cells was abolished by the excess of antigenic recombinant hMlze protein (data not shown). Although the N-terminal region of hMlze contains two potential bipartite NLS, hMlze appeared to be located in the cytoplasm.

To examine whether the potential bipartite NLS of hMlze were active in living cells, we ligated GFP cDNA upstream from the translation start codon in an in-frame manner and introduced the resulting plasmid construct into 293T and COS-7 cells. Consistent with the results of immunostaining, GFP-fused hMlze was located diffusely

in the cytoplasm of living cells (Fig. 6). Then, the subregions of hMlze polypeptide of interest were tagged to GFP and subcellular localization was examined in the same manner. First, hMlze was divided into two; the N-terminal half and C-terminal half of the protein. The C-terminal half of hMlze containing a leucine zipper (GFP-fused hMlze- Δ C in Fig. 5) was distributed equally in the cytoplasm and nucleus, whereas the N-terminal half of hMlze containing two potential bipartite NLS (GFP-fused hMlze- Δ N in Fig. 5) was located diffusely in the cytoplasm (Fig. 5C). Then the NLS sequence was examined for subcellular localization. GFP-fused hMlze-NLS2, the bipartite NLS second from the N-terminus of hMlze, was

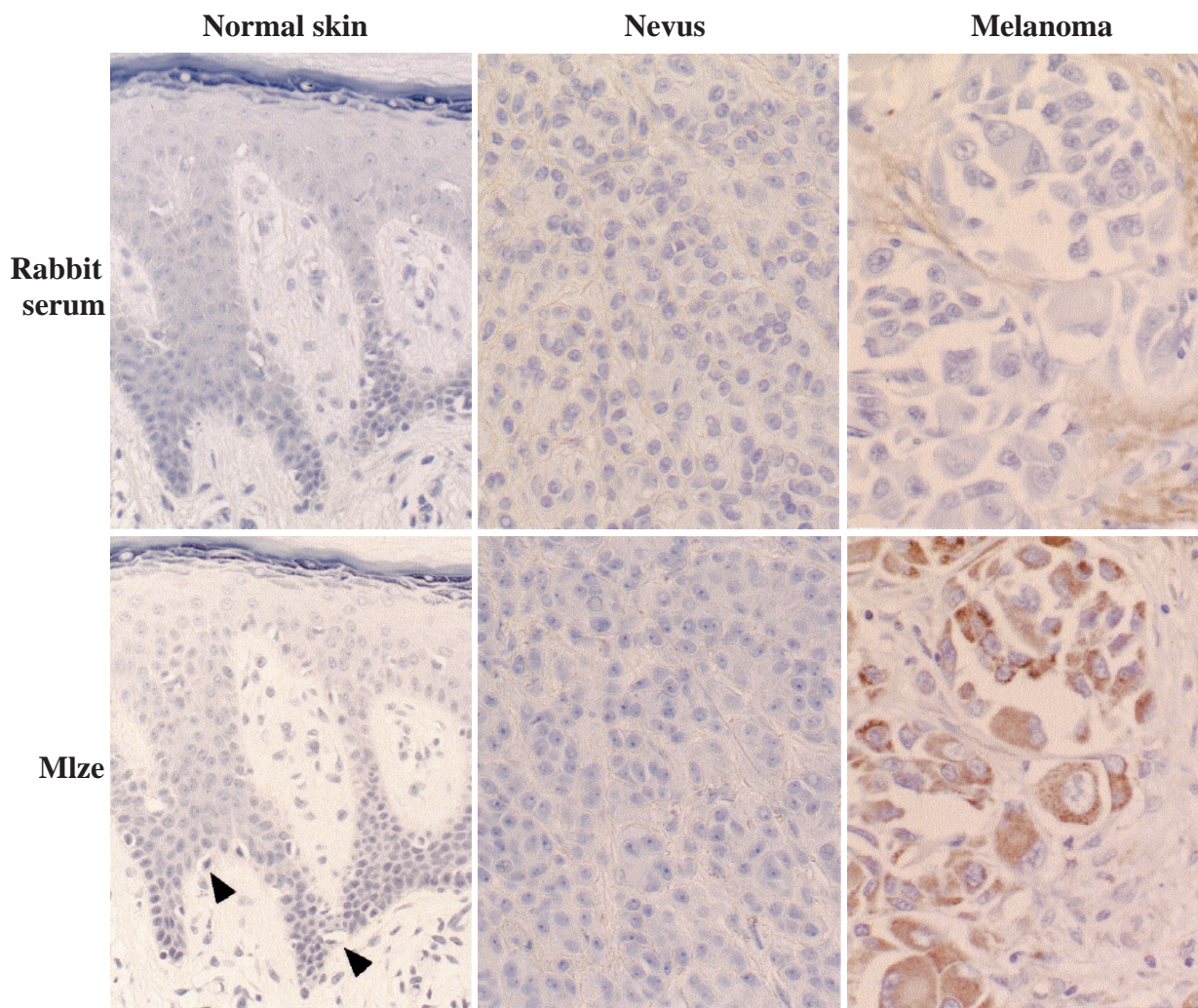


Fig. 7. Immunohistochemical staining of normal skin, nevus and melanoma. Samples were probed with anti-hMlze antibody (lower panel) or non-immunized normal IgG for control staining (upper panel). All samples were counterstained with hematoxylin. Melanocytes in the normal skin (arrow) and nevus cells were negative for staining, whereas melanoma cells showed cytoplasmic staining (original magnification $\times 10$ for normal skin and $\times 40$ for nevus and melanoma).

Table I. Clinical and Immunohistochemical Profile of Malignant Melanoma Patients

Progression phase	Case No.	Sex/age	Primary site	Diameter (cm)	Cell morphology	Pigmentation	Clark invasion level	hMlze expression				c-Myc expression					
								Epidermis	Papillary dermis	Reticular dermis	Subcutaneous fat	Epidermis	Papillary dermis	Reticular dermis	Subcutaneous fat		
RGP	1	F/58	sole	NI	epithelioid	moderate	I	(-)					(-)				
	2	M/63	sole	NI	epithelioid	mild	I	(-)					(-)				
	3	M/42	leg	NI	epithelioid	mild	I	(-)					(-)				
	4	F/74	sole	NI	epithelioid	mild	I	(-)					(-)				
	5	M/70	sole	NI	epithelioid	mild	I	(-)					(-)				
	6	F/30	arm	NI	epithelioid	moderate	I	(+)					(-)				
	7	F/30	finger	NI	mixed	moderate	I	(-)					(-)				
	8	M/52	sole	NI	epithelioid	moderate	I	(-)	(-)				(-)	(-)			
	9	F/52	sole	1.0	epithelioid	moderate	II	(-)	(-)				(-)	(-)			
	10	F/59	finger	1.0	epithelioid	moderate	II	(-)	(-)				(-)	(-)			
	11	M/56	arm	0.4	epithelioid	moderate	II	(-)	(-)				(+)	(+)			
	12	F/43	toe	1.0	epithelioid	moderate	II	(+)	(+)				(-)	(-)			
	13	M/66	sole	0.5	epithelioid	moderate	II	(-)	(-)				(+)	(+)			
	14	M/56	sole	NI	epithelioid	mild	II	(-)	(-)				(-)	(-)			
	15	M/61	sole	0.6	epithelioid	mild	II	(-)	(-)				(+)	(+)			
VGP	16	F/60	sole	0.8	epithelioid	no	III	(+)	(+)				(-)	(-)			
	17	M/54	sole	0.5	epithelioid	moderate	III	(-)	(-)				(-)	(-)			
	18	M/49	abdomen	2.1	epithelioid	no	III	(+)	(+)				(-)	(-)			
	19	F/54	sole	0.9	epithelioid	mild	III	(+)	(+)				(+)	(-)			
	20	F/49	sole	0.4	spindle	no	IV	(-)	(-)	(-)			(+)	(+)	(+)		
	21	F/45	toe	1.5	spindle	mild	IV	(+)	(+)	(+)			(-)	(-)	(-)		
	22	M/10	back	3.0	epithelioid	mild	IV	(-)	(-)	(-)			(+)	(+)	(+)		
	23	F/54	sole	0.9	epithelioid	moderate	IV	(-)	(-)	(-)			(-)	(-)	(-)		
	24	M/57	hand	0.8	spindle	moderate	IV	(-)	(+)	(+)			(-)	(-)	(-)		
	25	F/58	leg	2.0	epithelioid	mild	IV	(-)	(-)	(-)			(-)	(-)	(-)		
	26	M/41	sole	0.8	mixed	mild	V	(-)	(+)	(+)	(+)		(+)	(+)	(+)	(+)	

hMlze and c-Myc expression is judged at every level of the dermis; epidermis, papillary dermis, reticular dermis and subcutaneous fat. Diameter, diameter of the primary tumor; NI, not informative; mixed, mixed cell morphology with epithelioid- and spindle-shaped cells; (-), negative staining; (+), positive staining; shaded area; no data available.

predominantly located in the nucleus. These data suggest that the potential bipartite NLS of hMlze was functional but other regions present in the N-terminal half portion prevented hMlze from entering the nucleus.

Expression of hMlze and c-Myc in RGP and VGP melanoma Expression of hMlze was examined by immunohistochemistry in normal skin, nevi, and melanomas. Paraffin-embedded tissue samples were stained with anti-hMlze antibody and counterstained with hematoxylin. Control samples from each section were run using non-immunized rabbit serum instead of the primary antibody and counterstained with hematoxylin. Within normal skin, melanocytes were negative for hMlze (Fig. 7), which might be consistent with the fact that the hMLZE mRNA expression was not detectable in melan-a cells (Fig. 1). Nevus cells were negative for hMlze in five cases with intradermal nevus (Fig. 7).

hMlze expression was then examined in clinical cases of malignant melanoma. Clinical profiles are summarized

in Table I. Based upon Clark invasion level, twenty-six patients were divided into two groups; RGP melanoma group and VGP melanoma group. The former group was made up of fifteen cases of Clark I and II, while the latter was made up of eleven cases of Clark III, IV and V. In the VGP melanoma group, six out of eleven cases showed an hMlze-positive staining. In contrast, only two out of fifteen cases belonging to RGP melanoma group were positive for hMlze. The ratios of numbers of patients positive versus negative for hMlze were 6/11 and 2/15 in the VGP and RGP melanoma group, respectively. The difference between the two groups was significant by Fisher's exact and χ^2 tests ($P < 0.05$).

c-myc is one of the genes whose expression has been examined intensively in malignant melanoma.^{21, 22} In addition, we found that the c-myc gene is located in the neighborhood of the hMLZE gene. Hence, we examined whether c-Myc was also positive in the hMlze-positive melanoma samples. Other sections of melanoma samples were

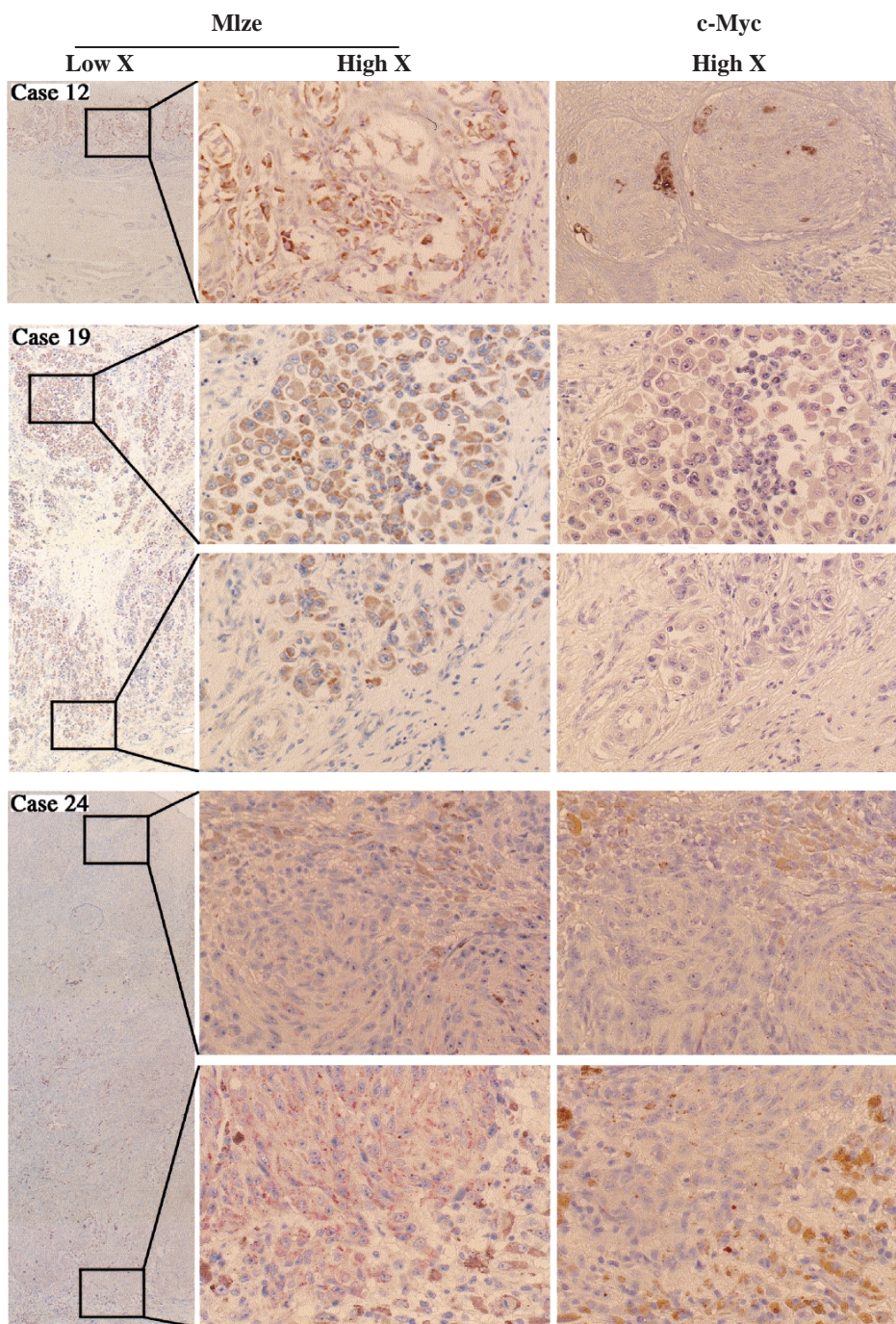


Fig. 8. Immunohistochemistry of human melanoma with anti-hMlze and anti-c-Myc antibody. The samples were stained with each antibody and counterstained with hematoxylin. Upper panel: one case of Clark invasion level II melanoma (case 12) positive for hMlze expression and negative for c-Myc expression. Middle panel: one case of Clark invasion level III melanoma (case 19) positive for expression of both hMlze and c-Myc. Overview of hMlze staining in low magnification. Upper and lower dermal components (boxes) of the tumor are shown in high magnification. The strength of c-Myc-staining substantially decreased at the lower component of tumor, whereas staining for hMlze was similar in both components. Lower panel: one case of Clark invasion level IV melanoma (case 24) positive for hMlze and negative for c-Myc. With AEC as a substrate for visualization, the red-brown staining for hMlze was distinguishable from the black-brown melanotic pigment. The strength of hMlze staining increased at the lower component of tumor. (Low X, original magnification $\times 4$; High X, original magnification $\times 20$) (original magnification $\times 20$).

stained with anti-c-Myc antibody. In the VGP melanoma group, four out of eleven cases showed c-Myc-positive staining. In contrast, three out of fifteen cases belonging to the RGP melanoma group were positive for c-Myc. The ratios of numbers of patients positive versus negative for c-Myc were 4/11 and 3/15 in the VGP and RGP melanoma group, respectively. The difference between the two groups was not significant by Fisher's exact and χ^2 tests ($P > 0.05$).

Histologic distribution of hMlze and c-Myc immunoreactivity in melanoma spread Immunoreactivity for hMlze and c-Myc was examined at each anatomic level of the melanoma spread; epidermis level, papillary dermis level, reticular dermis level and subcutaneous fat level. The results are summarized in Table I. None of six hMlze-positive cases (cases 16, 18, 19, 21, 24 and 26) in the VGP melanoma group showed a decrease in immunoreactivity to hMlze within the lower invasive component of the tumor. Moreover, in cases 24 and 26, the strength of hMlze staining increased at the lower invasive component of the tumor (case 24 in Fig. 8; case 26, data not shown). By contrast, in case 19, c-Myc-staining substantially decreased at the lower invasive component of the tumor, although it was detectable in melanoma cells resident in the upper component of the tumor (Fig. 8).

DISCUSSION

In an attempt to seek novel genes that are expressed differently between B16-F10 and B16-BL6 cells, we applied a method for constructing subtracted cDNA libraries. After subtraction of the B16-BL6 cDNA library with B16-F10 mRNA, we isolated a novel cDNA, mMLZE. Expression levels of mMLZE increased as B16 melanoma cells become more metastatic, and reached a peak in B16-BL6 cells (Fig. 1). Human homolog of MLZE (hMLZE) was isolated from a HeLa cDNA library. Among various systemic organs, hMLZE was expressed predominantly in trachea and spleen, suggesting a limited expression of hMLZE gene under physiological conditions. The hMlze protein contains a leucine zipper structure and two potential NLS. These structural features of hMlze may suggest that hMlze functions as a transcription factor in the nucleus. In fact, hMlze appeared to be present mainly in the cytoplasm under standard culture conditions. However, there is a possibility that hMlze may enter the nucleus under certain physiologic or pathologic conditions, since the bipartite NLS of hMlze were functional in nuclear translocation.

Both the hMLZE and c-myc genes are located in chromosome 8q24.1–2 region. The genomic region including 8q24.1–2 is amplified frequently not only in cutaneous melanoma,²³ but also in various cancers including ovarian cancer,²⁴ brain tumor,²⁵ breast cancer,²⁶ and lung can-

cer.²⁷ Since there was a possibility that hMLZE gene was amplified together with c-myc, we compared the expression of hMlze with that of c-Myc in human melanoma samples. Two of seven (29%) c-Myc positive samples co-expressed hMlze, while hMlze is expressed in about 30% of all melanoma samples examined in this study. In addition, the histologic distribution of immunoreactivity to hMlze was distinct from that to c-Myc when double-positive samples (case 19 in Fig. 8; case 26, data not shown) were examined. The DNA copy number of mouse and human MLZE was also investigated by Southern hybridization. However, no change in DNA copy number of MLZE gene was detected in mouse B16 sublines. Similar results were obtained with human lung cancer tissue, which expressed high levels of hMLZE (Watabe *et al.*, unpublished data). Upregulation of hMlze might not depend upon gene amplification, different from the case of c-Myc.²⁸

Although the function of Mlze remains unknown, its expression profiles and chromosomal localization suggested an involvement of Mlze in melanoma progression. In order to examine hMlze expression in human melanoma lesions and its correlation with malignant potentials, we divided malignant melanoma samples into two groups; RGP and VGP melanoma groups. Specimens of both groups were subjected to immunohistochemistry with anti-hMlze. The expression of c-Myc has been intensively investigated in melanocytic lesions.^{21,22} For comparison, specimens were also stained with c-Myc. The VGP melanoma group showed a positive immunoreactivity to hMlze at a significantly larger frequency than the RGP melanoma group. In contrast, there was no significant difference between the two groups in the frequency of positive immunoreactivity to c-Myc. The number of c-Myc-positive cases was smaller than that of hMlze-positive cases in VGP groups. In addition, we examined hMlze expression in nevus cells. Although nevus cells were reported to be often positive for c-Myc,²² all nevus specimens examined were negative for hMlze. Taken together, hMlze appeared to be more specific for malignant melanoma cells than c-Myc, and hMlze-specificity was stronger in advanced melanoma cells.

Several markers, such as HMB45 and c-Myc, are used to help diagnosis of malignant melanomas.²⁹ HMB45 is selective for malignant melanoma, while c-Myc is a broad marker for a number of human malignancies. HMB45 often fails to detect the lower invasive component of melanoma.³⁰ In fact, the strength of c-Myc-staining decreased substantially in the lower invasive component of case 19 (Fig. 8). We examined whether immunoreactivities for hMlze changed according to the invasive levels of melanoma cells. We did not find the strength of hMlze-staining to be decreased within the invasive descent of the melanoma spread. On the contrary, immunoreactivity for

hMlze increased remarkably as melanoma cells spread deeper into the dermis in case 24. These findings suggested that hMlze expression was upregulated in the course of melanoma progression from RGP to VGP. The anti-hMlze antibody could be useful to detect melanoma cells invading deepest into the dermis.

In the previous study we characterized annexin VII as a marker for less invasive phenotype of melanoma.¹⁵⁾ This gene was isolated from an F10 cDNA library subtracted with BL6 mRNA. In the present study, we isolated a novel gene, termed *MLZE*, from BL6 cDNA library subtracted with F10 mRNA. Immunohistochemistry of human melanoma lesions suggested that *MLze* was upregulated in the course of melanoma progression from RGP to VGP.

REFERENCES

- 1) Koh, H. K. Cutaneous melanoma. *N. Engl. J. Med.*, **325**, 171–182 (1991).
- 2) Barnhill, R. L., Mihm, M. C., Fitzpatrick, T. B. and Sober, E. J. Neoplasms: malignant melanoma. In "Dermatology in General Medicine," ed. T. B. Fitzpatrick, A. Z. Eisen, K. Wolff, I. M. Freedberg and K. F. Austen, pp. 1078–1116 (1993). McGraw-Hill, New York.
- 3) Clark, W. H., From, L., Bernardino, E. and Mihm, M. C. The histogenesis and biologic behavior of primary human malignant melanomas of the skin. *Cancer Res.*, **29**, 705–726 (1969).
- 4) Li, L., Price, J. E., Fan, D., Zhang, R. D., Bucana, C. D. and Fidler, I. J. Correlation of growth capacity of human tumor cells in hard agarose with their *in vivo* proliferative capacity at specific metastatic sites. *J. Natl. Cancer Inst.*, **81**, 1406–1412 (1989).
- 5) Albino, A. P. Genes involved in melanoma susceptibility and progression. *Curr. Opin. Oncol.*, **7**, 162–169 (1995).
- 6) Reed, A. J. and Albino, P. A. Update of diagnostic and prognosis markers in cutaneous malignant melanoma. *Dermatol. Clin.*, **17**, 631–643 (1999).
- 7) Breslow, A. Thickness, cross-sectional areas and depth of invasion in the prognosis of cutaneous melanoma. *Ann. Surg.*, **172**, 902–908 (1970).
- 8) Clark, W. H., Jr., Elder, D. E., Guerry, D., 4th, Braitman, L. E., Trock, B. J., Schultz, D., Synnestvedt, M. and Halpern, A. C. Model predicting survival in stage I melanoma based on tumor progression. *J. Natl. Cancer Inst.*, **24**, 1893–1904 (1989).
- 9) Hart, I. R. The selection and characterization of an invasive variant of the B16 melanoma. *Am. J. Pathol.*, **97**, 587–600 (1979).
- 10) Poste, G., Doll, J., Hart, I. R. and Fidler, I. J. B16 melanoma variants with enhanced tissue-invasive properties. *Cancer Res.*, **40**, 1636–1644 (1980).
- 11) Kobori, M., Ikeda, Y., Nara, H., Kato, M., Kumegawa, M., Nojima, H. and Kawashima, H. Large scale isolation of osteoclast-specific genes by an improved method involving the preparation of a subtracted cDNA library. *Genes Cells*, **3**, 459–475 (1998).
- 12) Ito, A., Kataoka, R. T., Watanabe, M., Nishiyama, K., Mazaki, Y., Sabe, H., Kitamura, Y. and Nojima, H. A truncated isoform of the PP2A B56 subunit promoted cell motility through paxillin phosphorylation. *EMBO J.*, **19**, 562–571 (2000).
- 13) Ito, A., Katoh, F., Kataoka, T. R., Okada, M., Tsubota, N., Asada, H., Yoshikawa, K., Maeda, S., Kitamura, Y., Yamasaki, H. and Nojima, H. A role of heterologous gap junctions between melanoma and endothelial cells in metastasis. *J. Clin. Invest.*, **105**, 1189–1197 (2000).
- 14) Nakaji, T., Kataoka, R. T., Watabe, K., Nishiyama, K., Nojima, H., Shimada, Y., Sato, F., Matsushima, H., Endo, Y., Kuroda, Y., Kitamura, Y., Ito, A. and Maeda, S. A new member of the GTPase superfamily that is upregulated in highly metastatic cells. *Cancer Lett.*, **147**, 139–147 (1999).
- 15) Kataoka, T. R., Ito, A., Asada, H., Watabe, K., Nishiyama, K., Nakamoto, K., Itami, S., Yoshikawa, K., Ito, M., Nojima, H. and Kitamura, Y. Annexin VII as a novel marker for invasive phenotype of malignant melanoma. *Jpn. J. Cancer Res.*, **91**, 75–83 (2000).
- 16) Bennett, C. D., Cooper, J. P. and Hart, R. I. A line of non-tumorigenic mouse melanocytes, syngeneic with the B16 melanoma and requiring a tumor promoter for growth. *Int. J. Cancer*, **39**, 414–418 (1987).
- 17) Endo, Y., Fujita, T., Tamura, K., Tsuruga, H. and Nojima, H. Structure and chromosomal assignment of the human cyclin G gene. *Genomics*, **38**, 92–95 (1996).
- 18) Fujii, T., Tamura, K., Copeland, G. N., Gilbert, J. D., Jenkins, A. N., Yomogida, K., Tanaka, H., Nishimune, Y., Nojima, H. and Abiko, Y. Sperizin is a murine RING zinc-finger protein specifically expressed in haploid germ cells. *Genomics*, **57**, 94–101 (1999).
- 19) Kozak, M. Compilation and analysis of sequences upstream from the translational start site in eukaryotic mRNAs. *Nucleic Acids Res.*, **12**, 857–872 (1984).
- 20) Dingwall, C. and Laskey, R. A. Nuclear targeting

- sequences—a consensus? *Trends Biochem. Sci.*, **16**, 478–481 (1991).
- 21) Lazaris, A. C., Theodoropoulos, G. E., Aroni, K., Saetta, A. and Davaris, P. S. Immunohistochemical expression of c-myc oncogene, heat shock protein 70 and HLA-DR molecules in malignant cutaneous melanoma. *Virchows Arch.*, **426**, 461–467 (1995).
 - 22) Bergman, R., Lurie, M., Kerner, H., Kilim, S. and Friedman-Birnbaum, R. Mode of c-myc protein expression in Spitz nevi, common melanocytic nevi and malignant melanomas. *J. Cutan. Pathol.*, **24**, 219–222 (1997).
 - 23) Bastian, C. B., LeBoit, E. P., Hamm, H., Brocjer, B. E. and Pinkel, D. Chromosomal gains and losses in primary cutaneous melanomas detected by comparative genomic hybridization. *Cancer Res.*, **58**, 2170–2175 (1998).
 - 24) Sonoda, G., Palazzp, J., du Manoir, S., Godwin, A. K., Feder, M., Yakushiji, M. and Testa, J. R. Comparative genomic hybridization detects frequent overrepresentation of chromosomal material from 3q26, 8q24, and 20q13 in human ovarian carcinomas. *Genes Chromosom. Cancer*, **20**, 320–328 (1997).
 - 25) Nishizaki, T., Ozaki, S., Harada, K., Ito, H., Arai, H., Beppu, T. and Sasaki, K. Investigation of genetic alterations associated with the grade of astrocytic tumor by comparative genomic hybridization. *Genes Chromosom. Cancer*, **21**, 340–346 (1998).
 - 26) Muleris, M., Almedia, A., Gerbault-Seureau, M., Malfoy, B. and Dutrillaux, B. Detection of DNA amplification in 17 primary breast carcinomas with homogeneously staining regions by a modified comparative genomic hybridization technique. *Genes Chromosom. Cancer*, **10**, 160–170 (1994).
 - 27) Testa, J. R., Liu, Z., Feder, M., Bell, D. W., Balsara, B., Cheng, J. Q. and Taguchi, T. Advances in the analysis of chromosome alterations in human lung carcinomas. *Cancer Genet. Cytogenet.*, **95**, 20–32 (1997).
 - 28) Bergh, J. C. Gene amplification in human lung cancer. The myc family genes and other proto-oncogenes and growth factor genes. *Am. Rev. Respir. Dis.*, **142**, 20–26 (1990).
 - 29) Gown, A. M., Vogel, A. M., Hoak, D., Gough, F. and McNutt, M. A. Monoclonal antibodies specific for melanocytic tumors distinguish subpopulations of melanocytes. *Am. J. Pathol.*, **123**, 195–203 (1986).
 - 30) King, R., Weilbaecher, K. N., McGill, G., Cooley, E., Mihm, M. and Fisher, D. E. Microphthalmia transcription factor. A sensitive and specific melanocyte marker for melanoma diagnosis. *Am. J. Pathol.*, **155**, 731–738 (1999).